Supplementary Material

for

Latonduine-1-Amino-Hydantoin Hybrid, Triazole-Fused Latonduine Schiff Bases and Their Metal Complexes: Synthesis, X-ray and Electron Diffraction, Molecular Docking Studies and Antiproliferative Activity

Christopher Wittmann [1], Tim Gruene [1], Alexander Prado-Roller [1], Sandra Aranđelović [2], Jóhannes Reynisson [3] and Vladimir B. Arion [1,*]

[1] Institute of Inorganic Chemistry of the University of Vienna, Währinger Strasse 42, A1090 Vienna, Austria

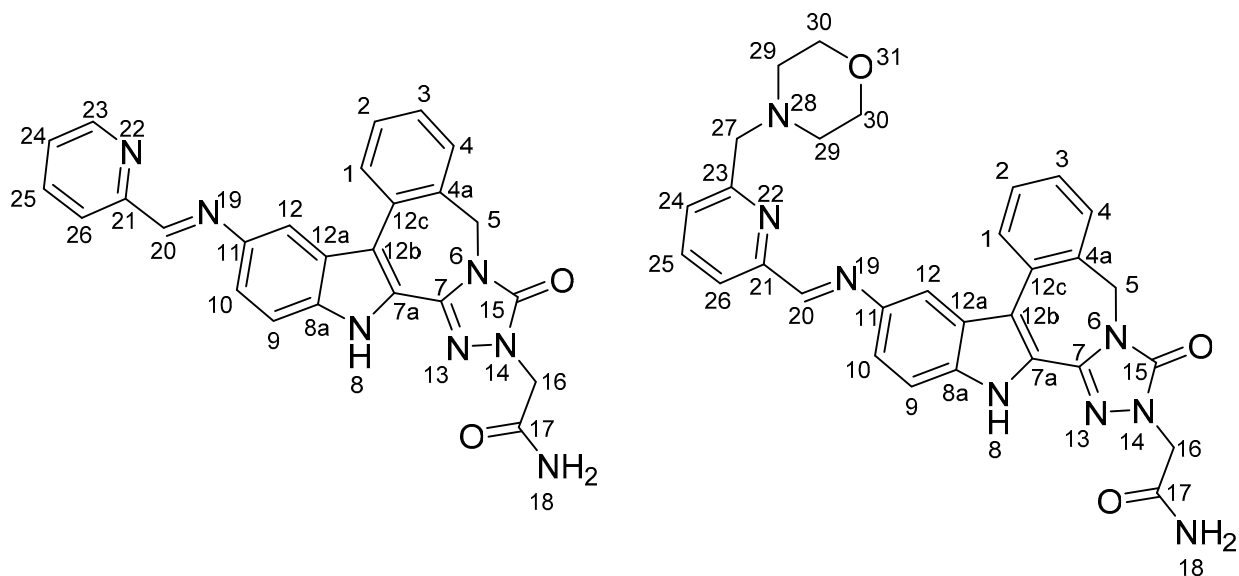[2] Institute of Oncology and Radiology of Serbia, Pasterova 14, 11000 Belgrade, Serbia

[3] School of Pharmacy and Bioengineering, Keele University, Hornbeam Building, Staffordshire ST5 5BG, UK
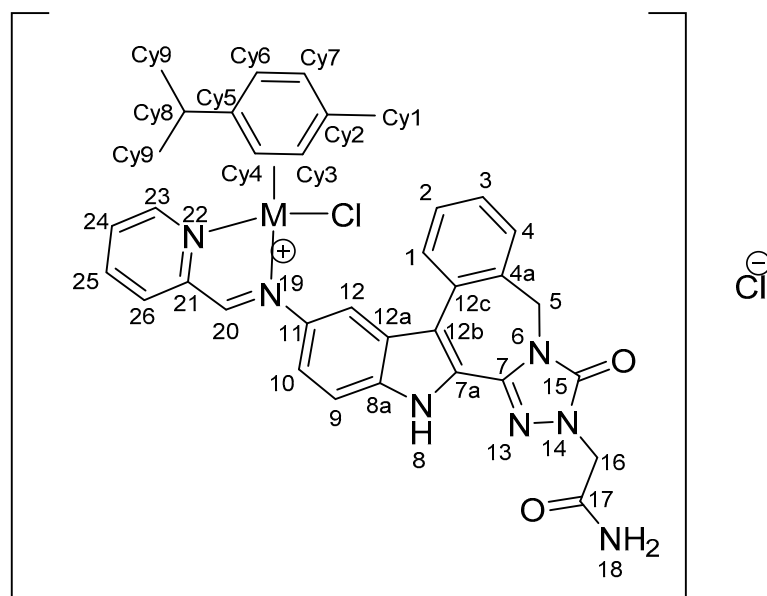
[*] Correspondence: vladimir.arion@univie.ac.at

Table of Contents

Numbering schemes

Scheme S1. Numbering scheme of **HL^1** and **HL^2**.

Scheme S2. Numbering scheme for complexes **1** (M = Ru) and **2** (M = Os).

Table S1. Yields and analytical data for **HL^1** and **HL^2**, and complexes **1**–**3**.

		B	HL^1	HL^2	1	2	3
Yield (%)		60	69	71	91	76	89
Brutto formula		C$_{19}$H$_{14}$N$_6$O$_4$-0.8H$_2$O-0.4CH$_3$OH	C$_{25}$H$_{19}$N$_7$O$_2$-1.1H$_2$O	C$_{30}$H$_{28}$N$_8$O$_3$-2H$_2$O	C$_{35}$H$_{33}$N$_7$O$_2$RuCl$_2$-2.5H$_2$O	C$_{35}$H$_{33}$N$_7$O$_2$OsCl$_2$-2.4H$_2$O	C$_{30}$H$_{28}$N$_8$O$_3$CuCl$_2$-H$_2$O·0.3C$_3$H$_8$O
M$_r$		417.58	469.28	584.62	800.69	888.05	719.09
C (%)	**calcd**	55.79	63.98	61.63	52.5	47.33	51.61
	found	55.92	63.78	61.85	52.52	47.65	51.51
H (%)	**calcd**	4.15	4.55	5.51	4.78	4.29	4.54
	found	3.98	4.3	5.21	4.52	4.05	4.35
N (%)	**calcd**	20.12	20.89	19.16	12.24	11.04	15.58
	found	19.76	20.71	19.26	11.85	11.01	15.36
O (%)	**calcd**			9.56		7.92	
	found			9.96		8.11	
ESI-MS	**[M + H]$^+$**	391.17	450.25	549.33			
	[M + Na]$^+$		472.22				
	[M - Cl]$^+$				720.21	810.26	646.2
X-ray structure		YES	YES				YES

Crystallographic data obtained from both X-ray diffraction and electron diffraction techniques

Table S2. Crystallographic data and refinement details for B·CH$_3$OH and HL^1·2DMF and 3.

Compound	**B·CH$_3$OH**	**HL^1·2DMF**	**3**
empirical formula	C$_{20}$H$_{18}$N$_6$O$_5$	C$_{31}$H$_{33}$N$_9$O$_4$	C$_{30}$H$_{28}$Cl$_2$CuN$_8$O$_3$
fw	422.40	595.66	683.05
space group	monoclinic, $C2/c$	triclinic, $P\bar{1}$	monoclinic, $P2_1/n$
a, Å	34.647(14)	8.7154(7)	11.16(3)
b, Å	11.809(5)	11.8767(10)	9.602(13)
c, Å	19.252(7)	15.5370(16)	26.92(7)
α,°	90	111.185(5)	90
β, °	98.83(2)	95.529(4)	94.6(5)
γ, °	90	90.420(4)	90
V [Å^3]	7784(5)	1491.0(2)	2877(11)
Z	16	2	4
λ [Å]	0.71073	0.71073	0.02508
ρ_{calcd}, g cm^{-3}	1.442	1.327	1.577
cryst size, mm^3	0.44 × 0.13 × 0.04	0.20 × 0.20 × 0.20	0.005 × 0.0013 × 0.0005
T [K]	100(2)	100(2)	148(1)
μ, mm^{-1}	0.107	0.092	
$R_1{}^a$	0.0616	0.0577	0.1985
$wR_2{}^b$	0.1569	0.1655	0.5049
GOF^c	0.956	1.011	1.514

^{a} $R_1 = \Sigma||F_o| - |F_c||/\Sigma|F_o|$. ^{b} $wR_2 = \{\Sigma[w(F_o{}^2 - F_c{}^2)^2]/\Sigma[w(F_o{}^2)^2]\}^{1/2}$. ^{c} GOF = $\{\Sigma[w(F_o{}^2 - F_c{}^2)^2]/(n - p)\}^{1/2}$, where n is the number of reflections and p is the total number of parameters refined.

Synthesis of *C**

To species **C** (225 mg, 0.61 mmol) in MeOH (20 mL) triethylamine (1 mL) was added. The solution was stirred at 80 °C for 3 h. The precipitate was filtered off after cooling to room temperature and washed with Et$_2$O (1 mL). The product was dried to give a light-beige solid. Yield: 156 mg. ^{1}H NMR (500 MHz, DMSO-d_6) δ 11.88 (s, 1H), 7.88 (t, J = 7.4 Hz, 1H), 7.56 (d, J = 7.4 Hz, 2H), 7.50 (td, J = 7.7, 1.2 Hz, 1H), 7.35 – 7.26 (m, 2H), 7.24 (t, J = 6.8 Hz, 1H), 7.14 (d, J = 1.7 Hz, 1H), 6.72 (dt, J = 11.8, 5.9 Hz, 1H), 4.81 (s, 2H), 4.69 (s, 2H), 4.36 (s, 2H).
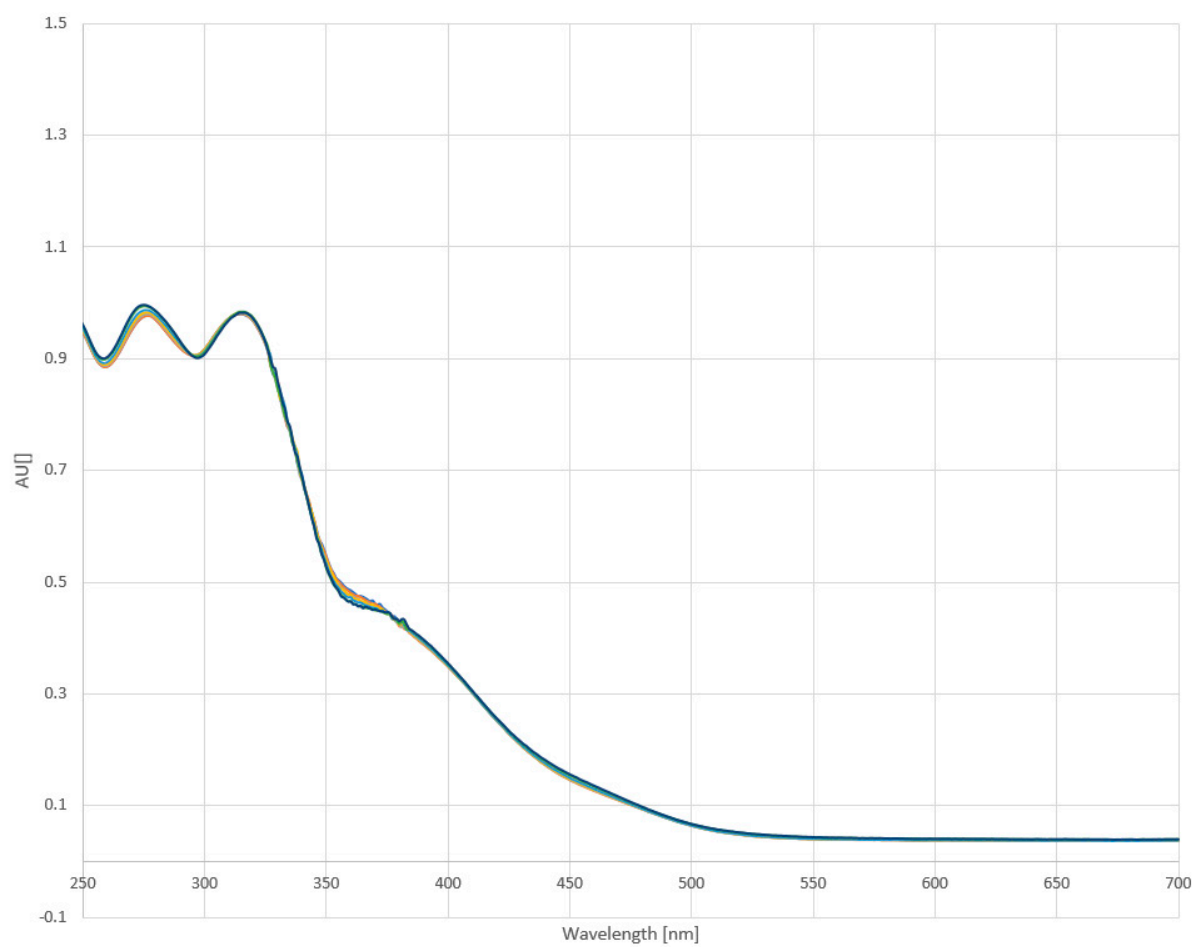
UV‒vis stability data

Figure S1. UV–vis absorption spectra of **1** (35 µM) in DMSO/H_2O 1/99 monitored over 72 h.
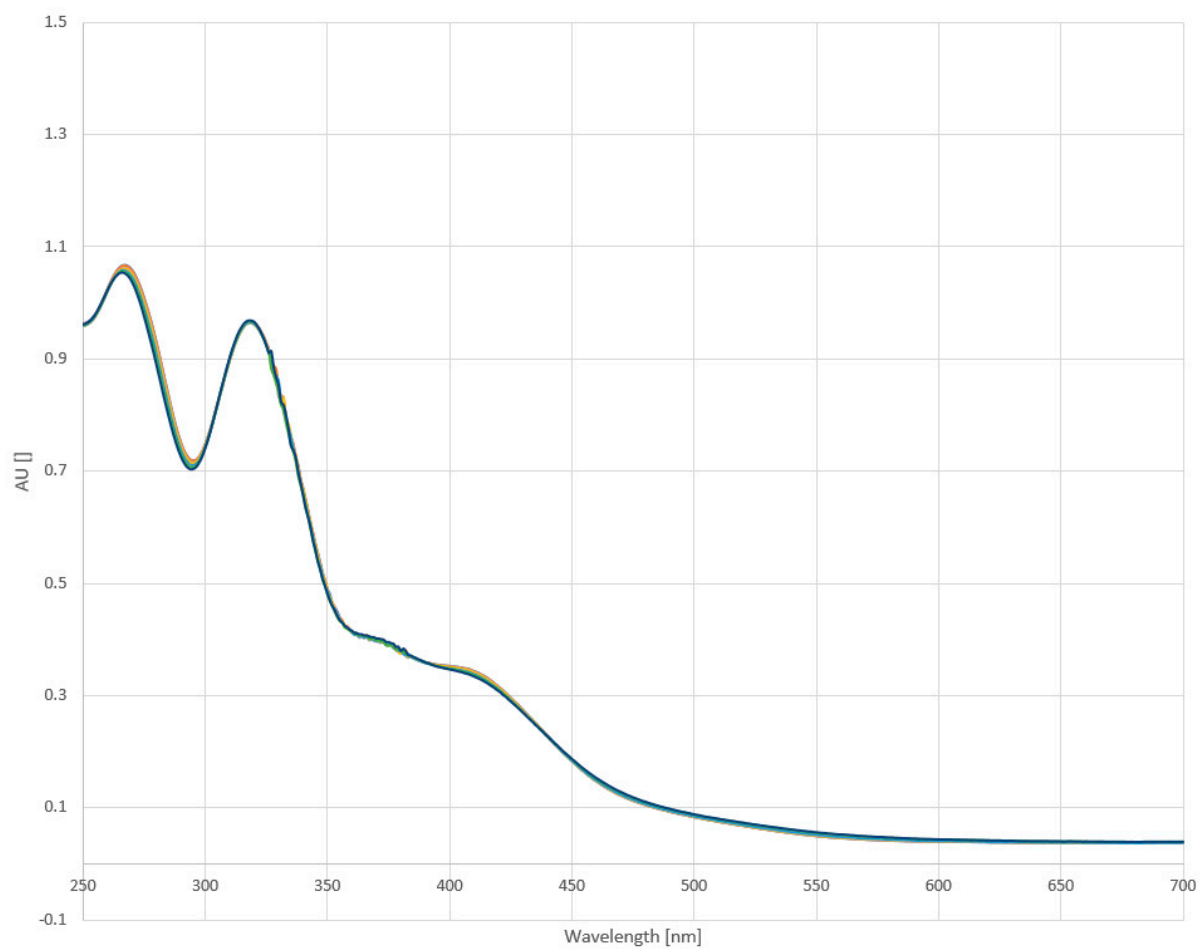
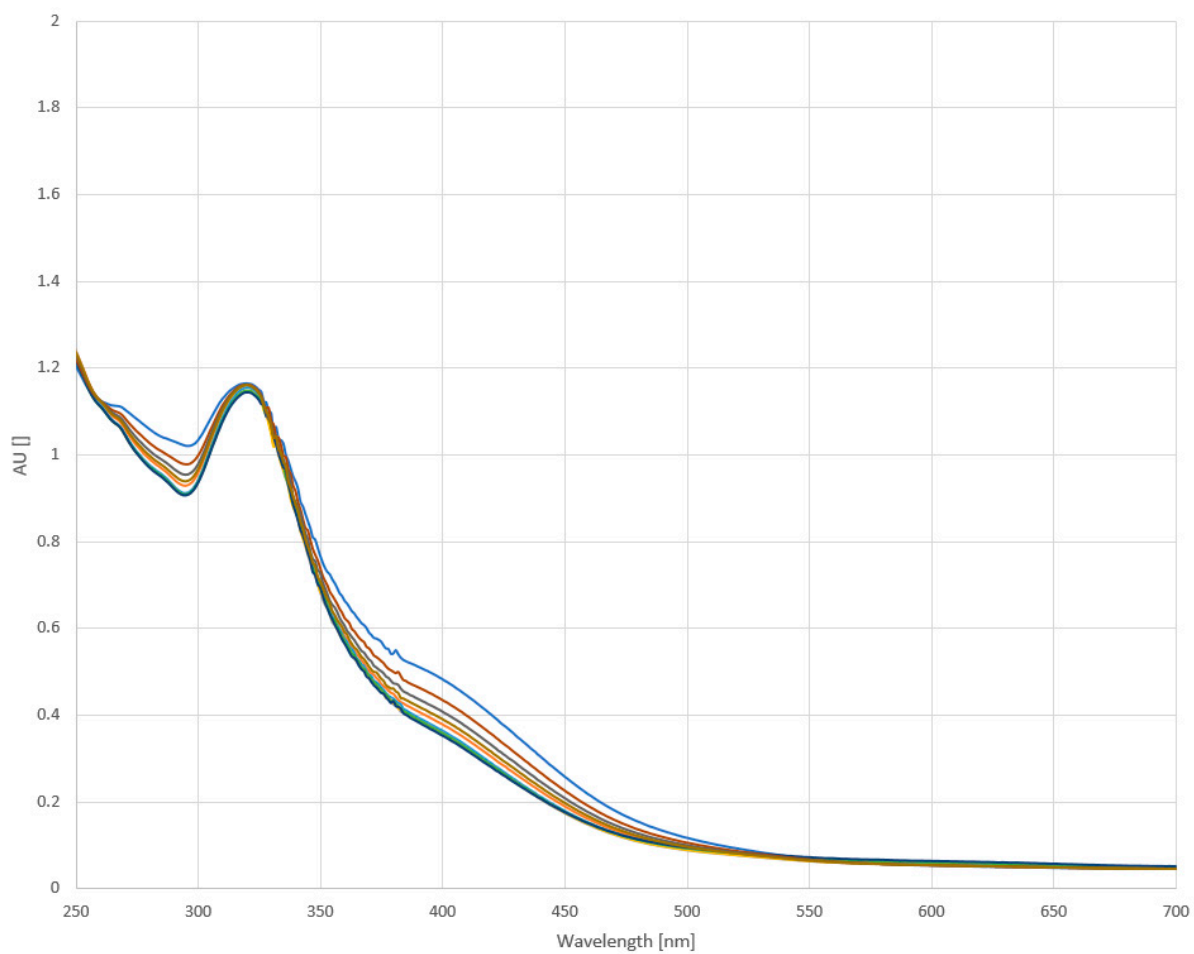**Figure S2.** UV–vis absorption spectra of **2** (37 μM) in DMSO/H_2O 1/99 monitored over 72 h.

Figure S3. UV–vis absorption spectra of **3** (49 µM) in DMSO/H_2O 1/99 monitored over 72 h.
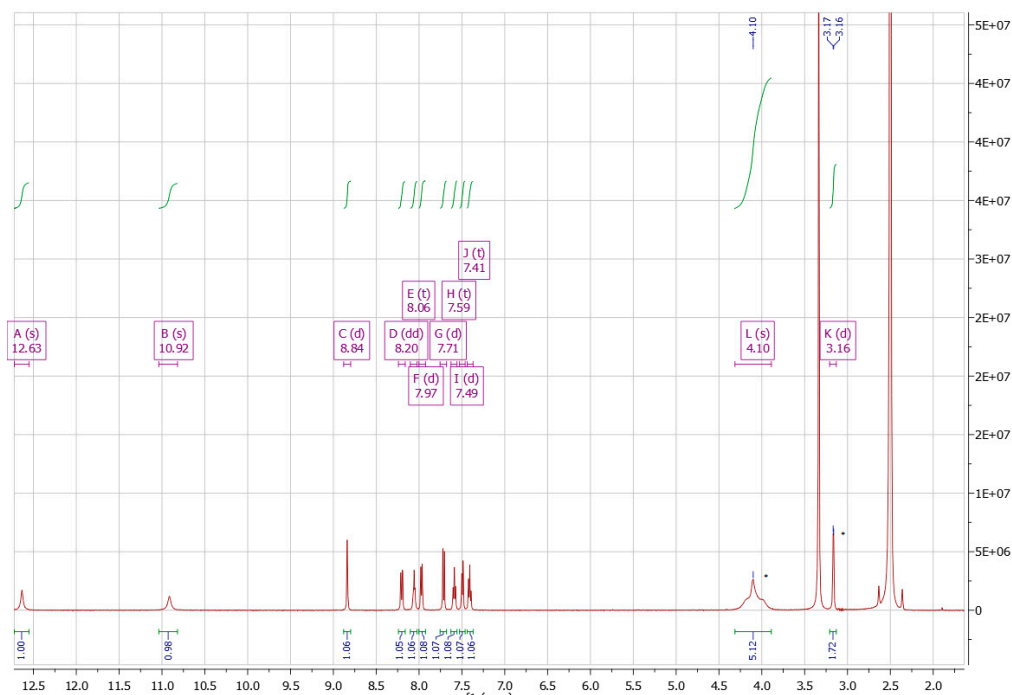
NMR spectra

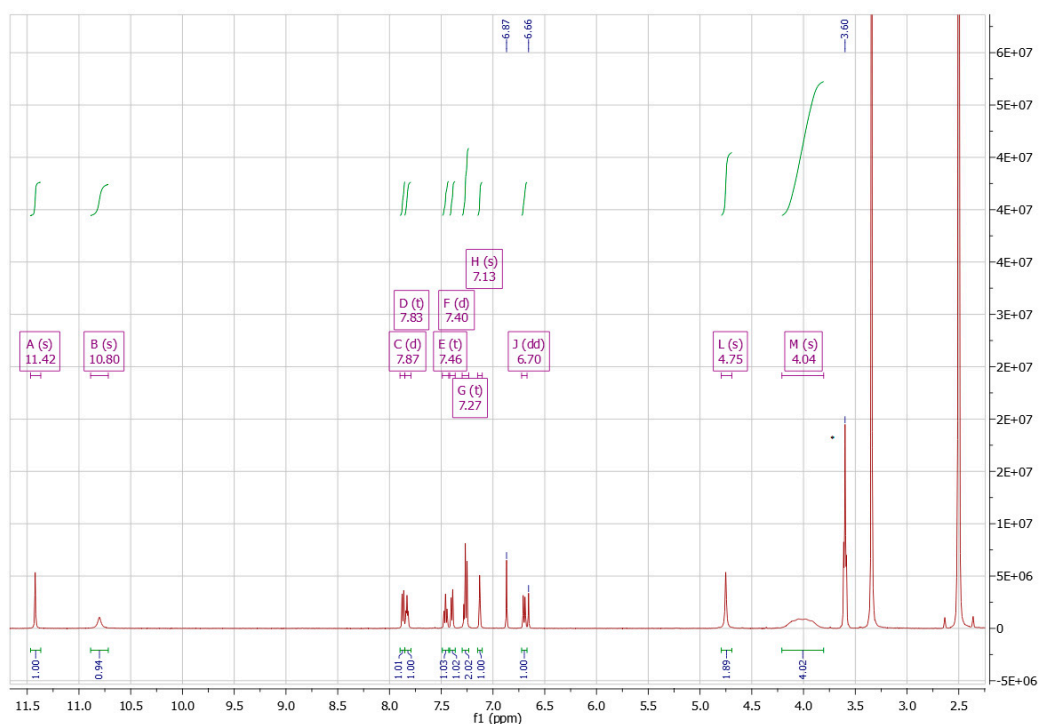**Figure S4.** ^{1}H NMR spectrum of **B**. Residual MeOH is marked with an asterisk (*).
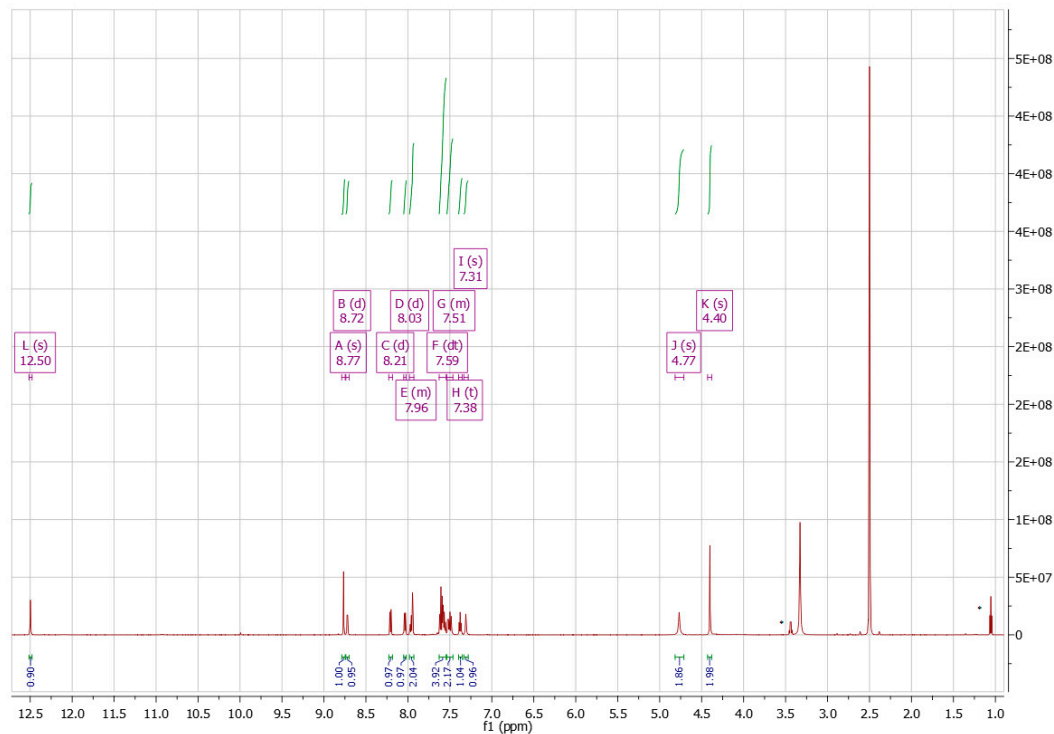

Figure S5. ^{1}H NMR spectrum of **C**. Residual THF is marked with an asterisk (*).
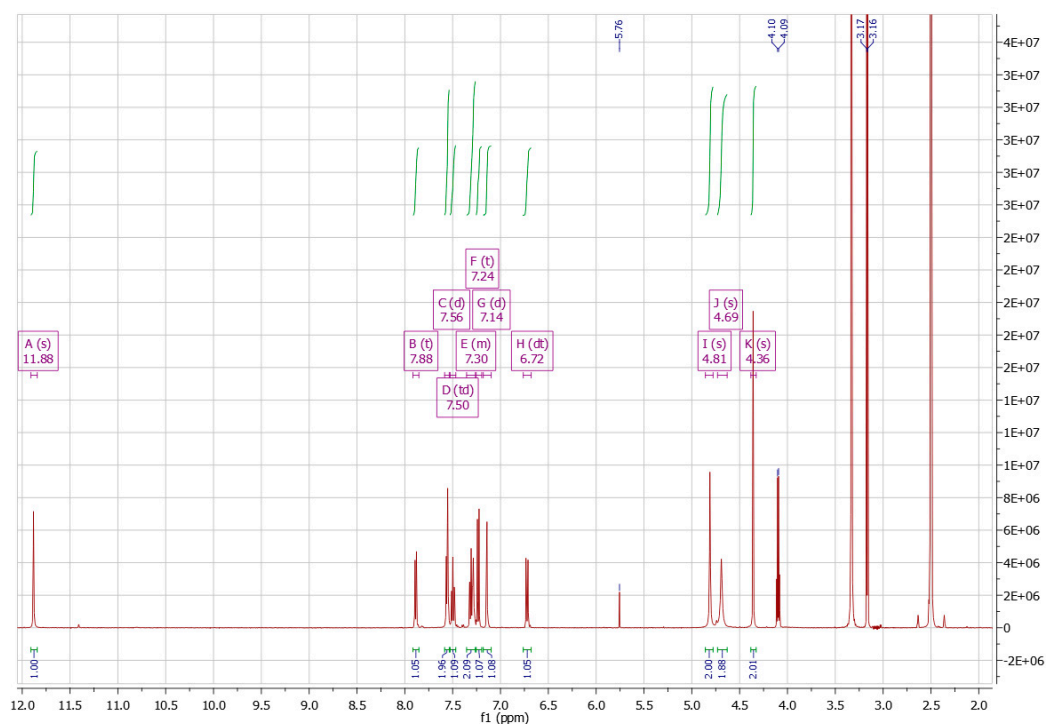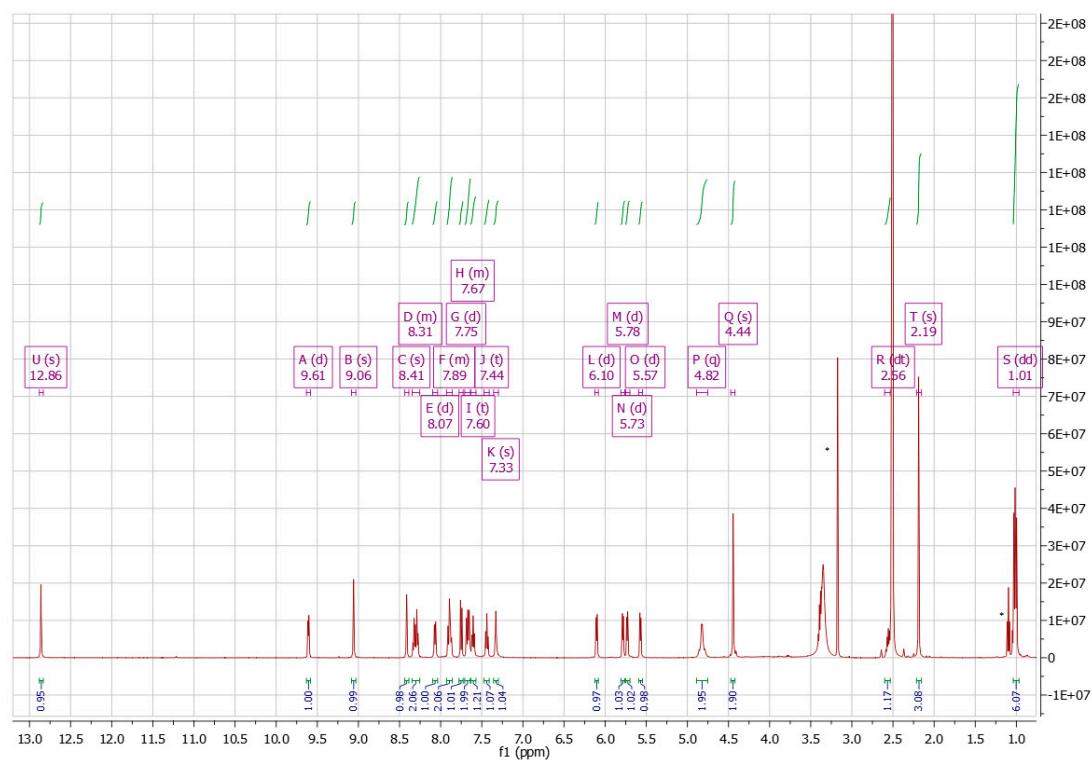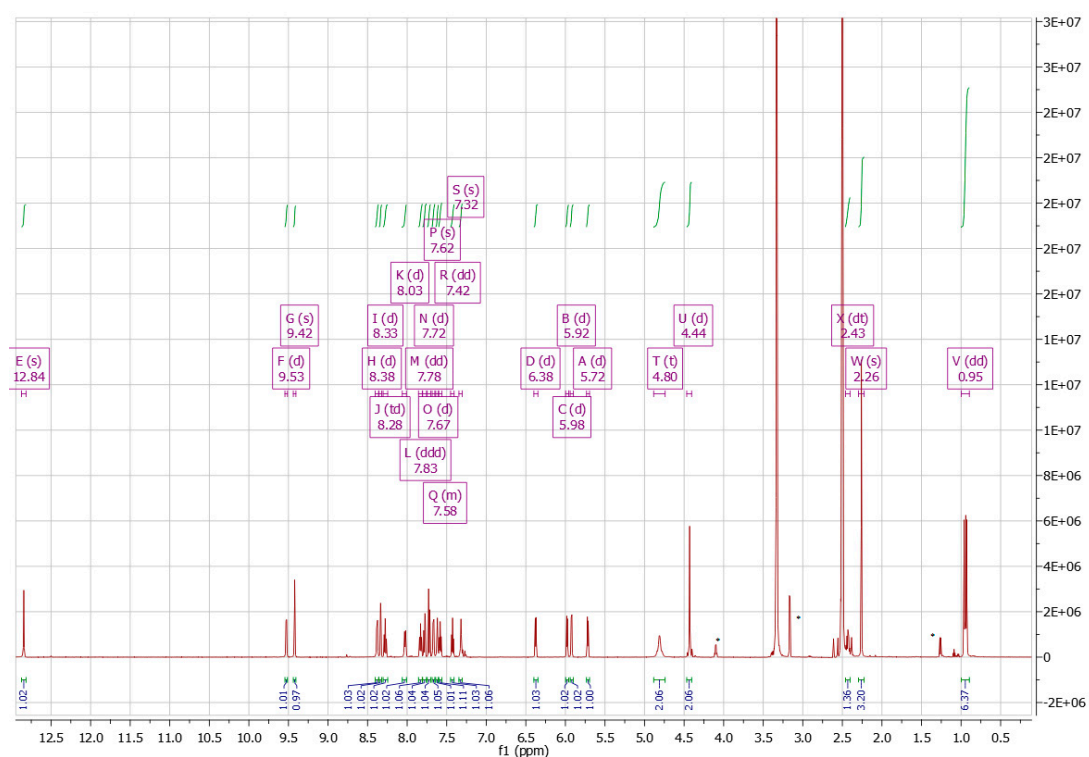
Figure S6. ^{1}H NMR spectrum of **C***. Residual solvents are identified by their respective chemical shifts on the top.

Figure S7. ^{1}H NMR spectrum of **HL**[1]. Residual EtOH is marked with an asterisk (*).

Figure S8. ¹H NMR spectrum of **HL²**. Residual EtOH is marked with an asterisk (*).

Figure S9. ¹H NMR spectrum of **1**. Residual ¹PrOH is marked with an asterisk (*).

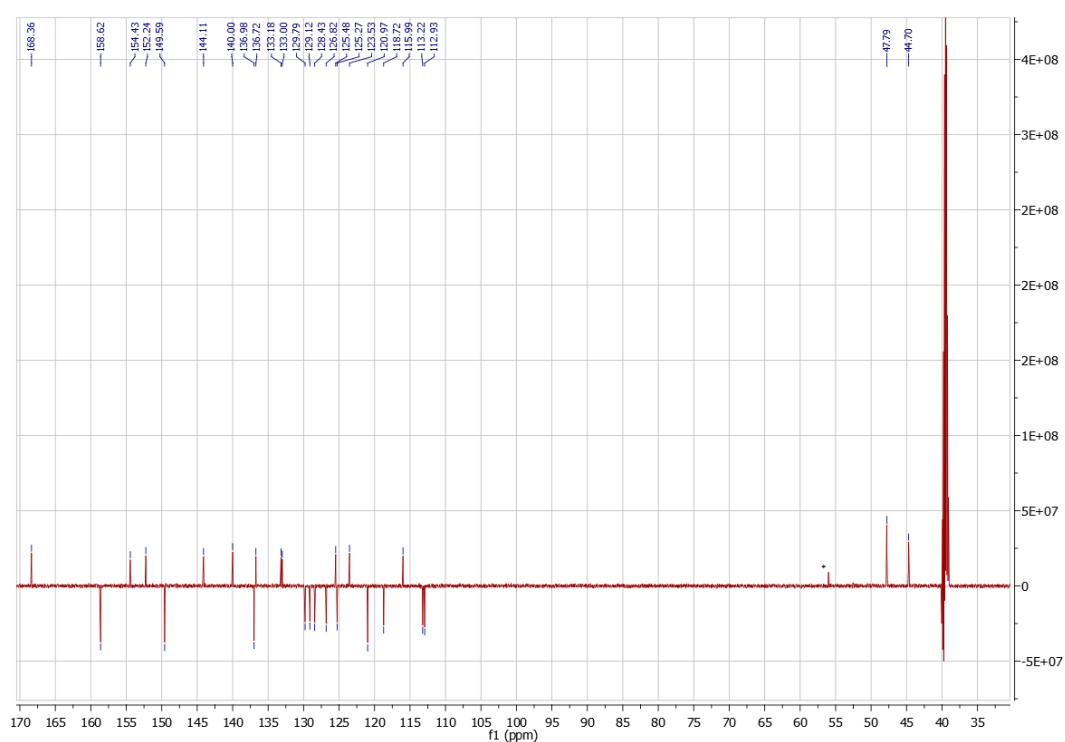**Figure S10.** ^{1}H NMR spectrum of **2**. Residual ^{i}PrOH is marked with an asterisk (*).

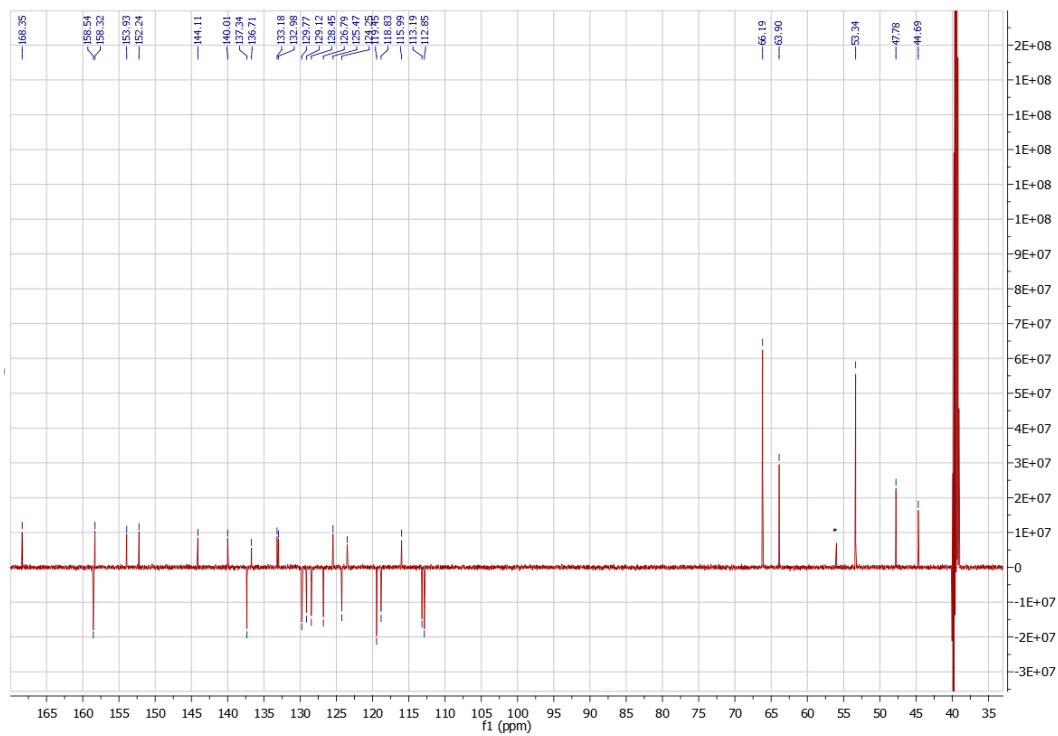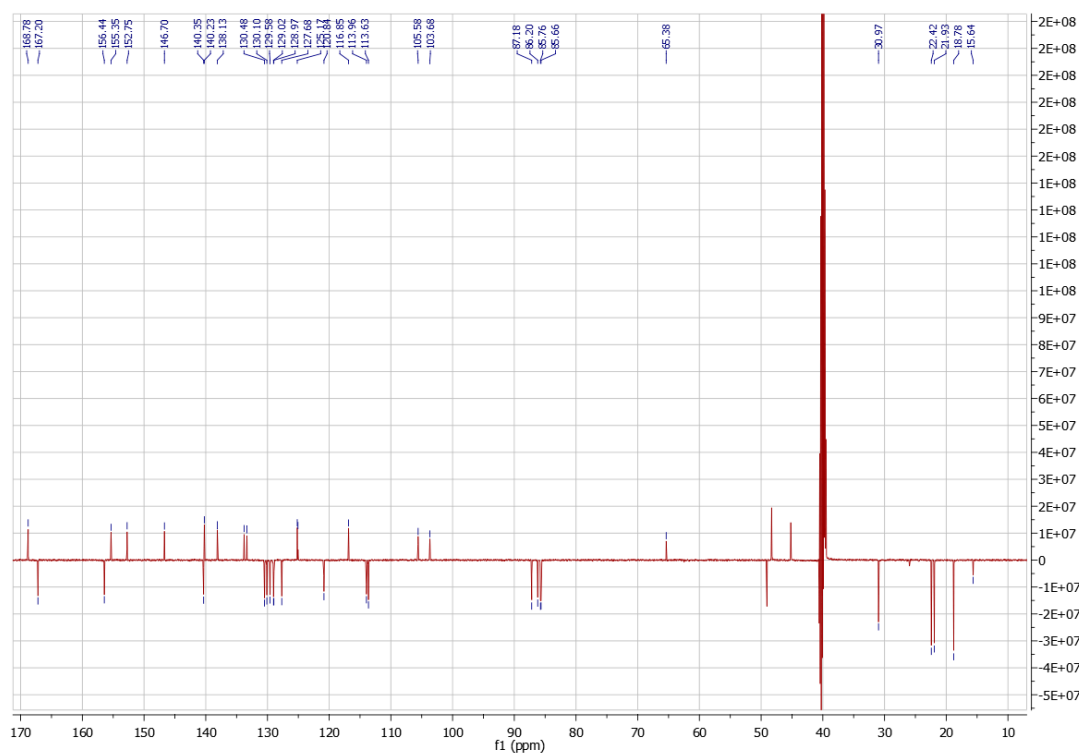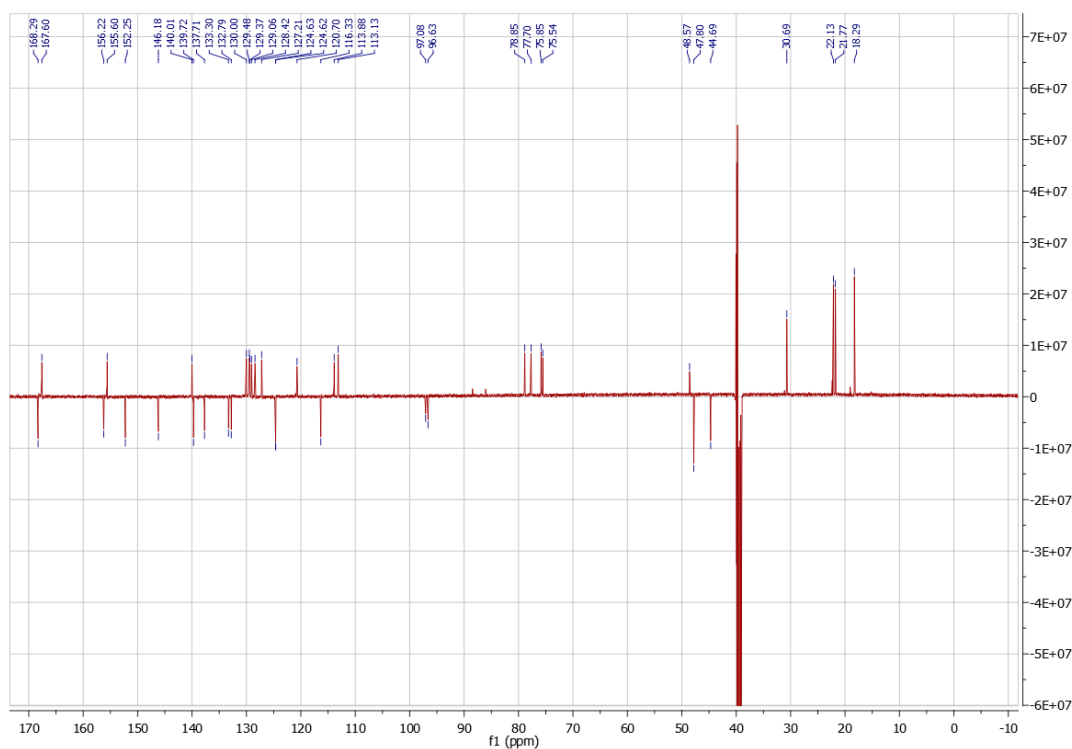**Figure S11.** ^{13}C NMR spectrum of **HL^1**. Residual EtOH is marked with an asterisk (*).

Figure S12. ^{13}C NMR spectrum of **HL^2**. Residual EtOH is marked with an asterisk (*).

Figure S13. ^{13}C NMR spectrum of **1**.
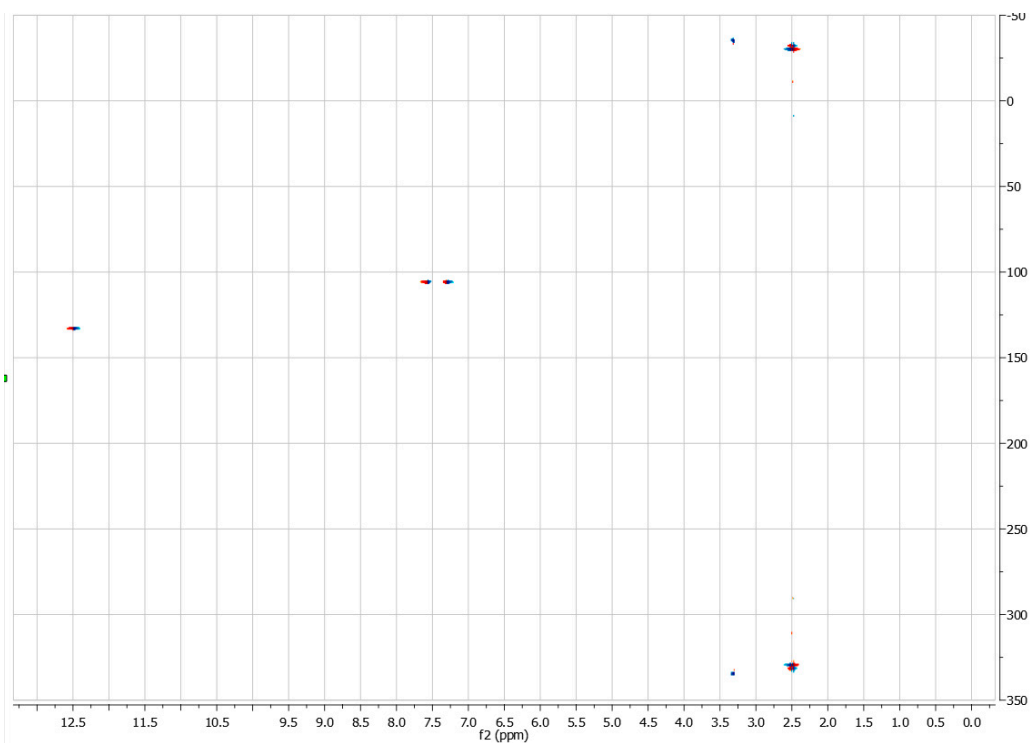
Figure S14. ^{13}C NMR spectrum of **2**.

Figure S15. ^{15}N-^{1}H HSQC NMR spectrum of **HL^1**.
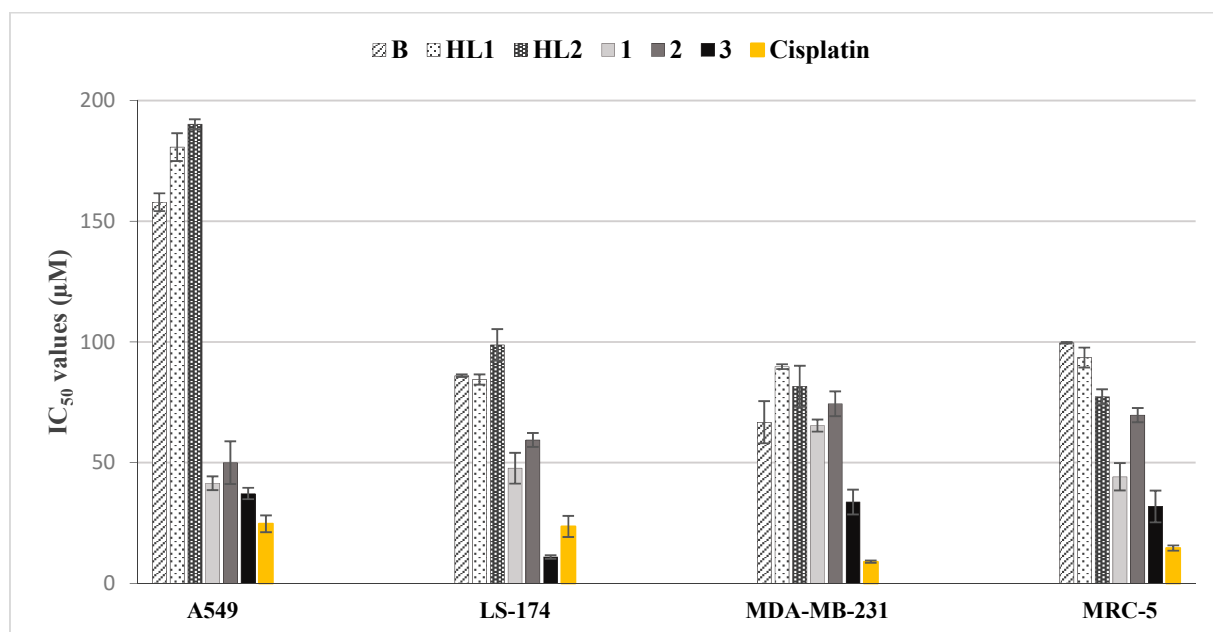
Antiproliferative Activity

Figure S16. Bar graphs present IC$_{50}$ values (µM) of tested complexes and ligands vs cisplatin in three human tumor cell lines (A549, LS-174, MDA-MB-231) and non-tumor MRC-5 cells. Each IC$_{50}$ value presents average of at least three independent experiments ± SD, obtained for 72 h action using MTT assay.
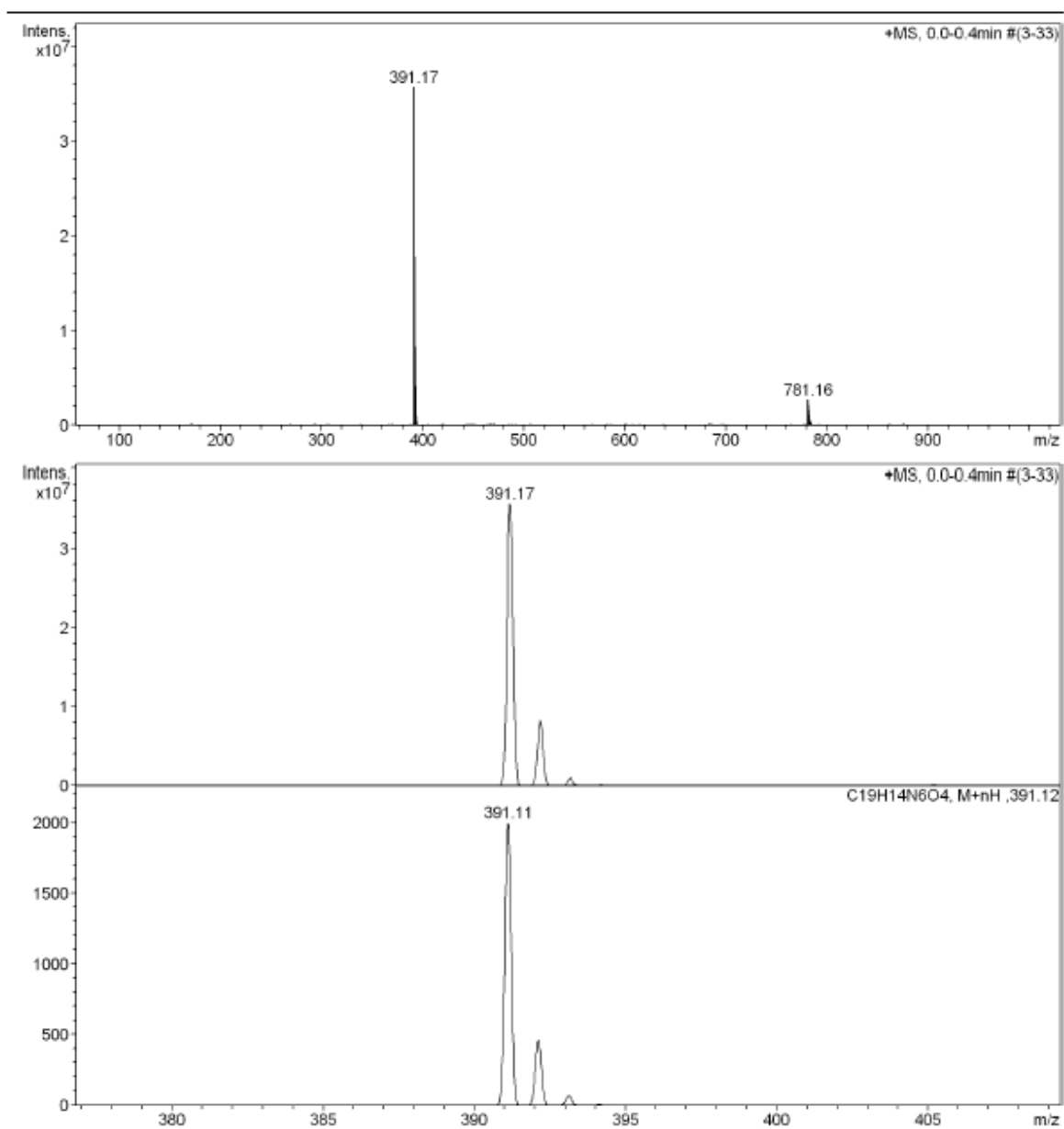
ESI-mass spectra

Figure S17. Positive ion ESI-mass spectrum of **B**.

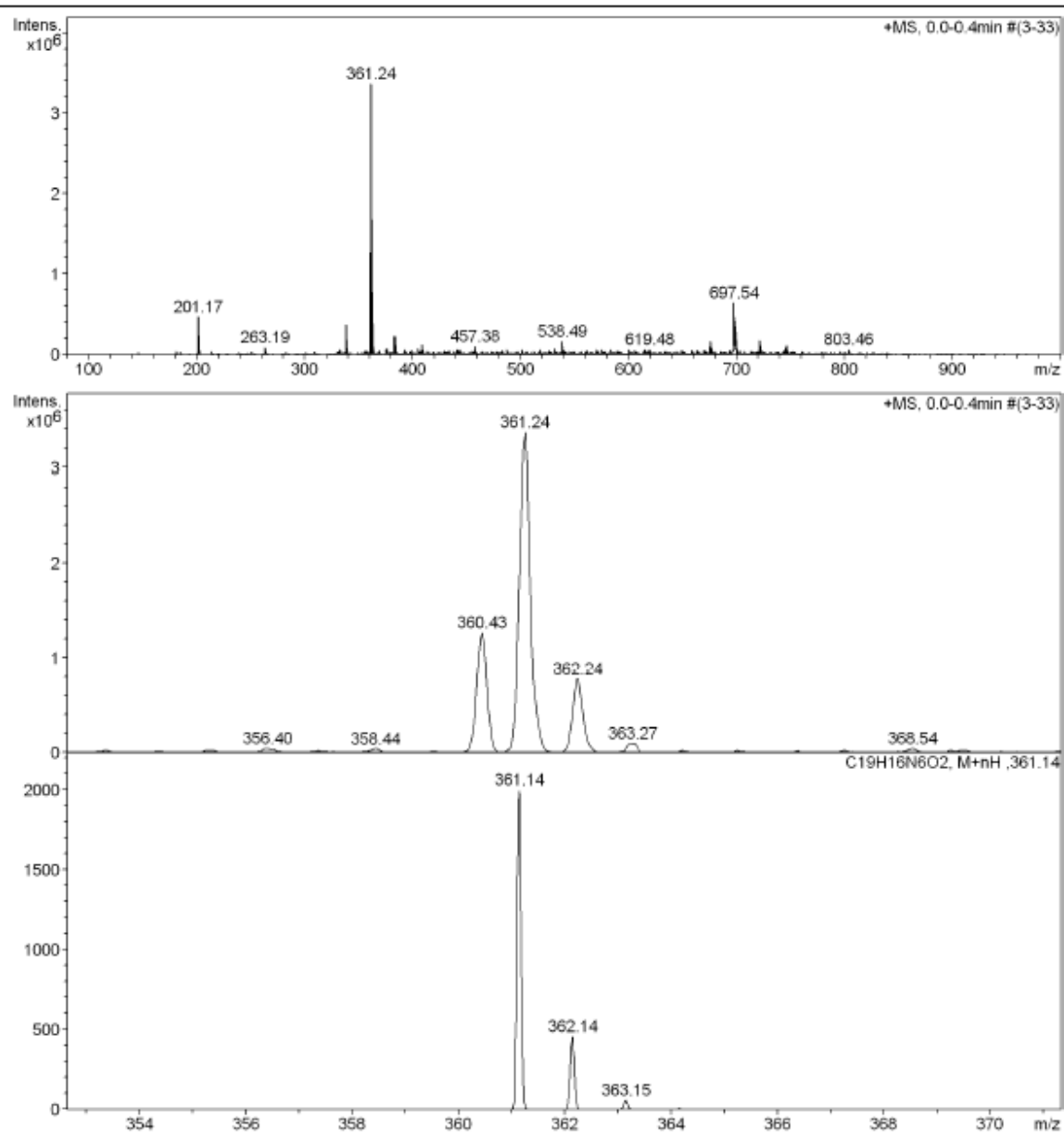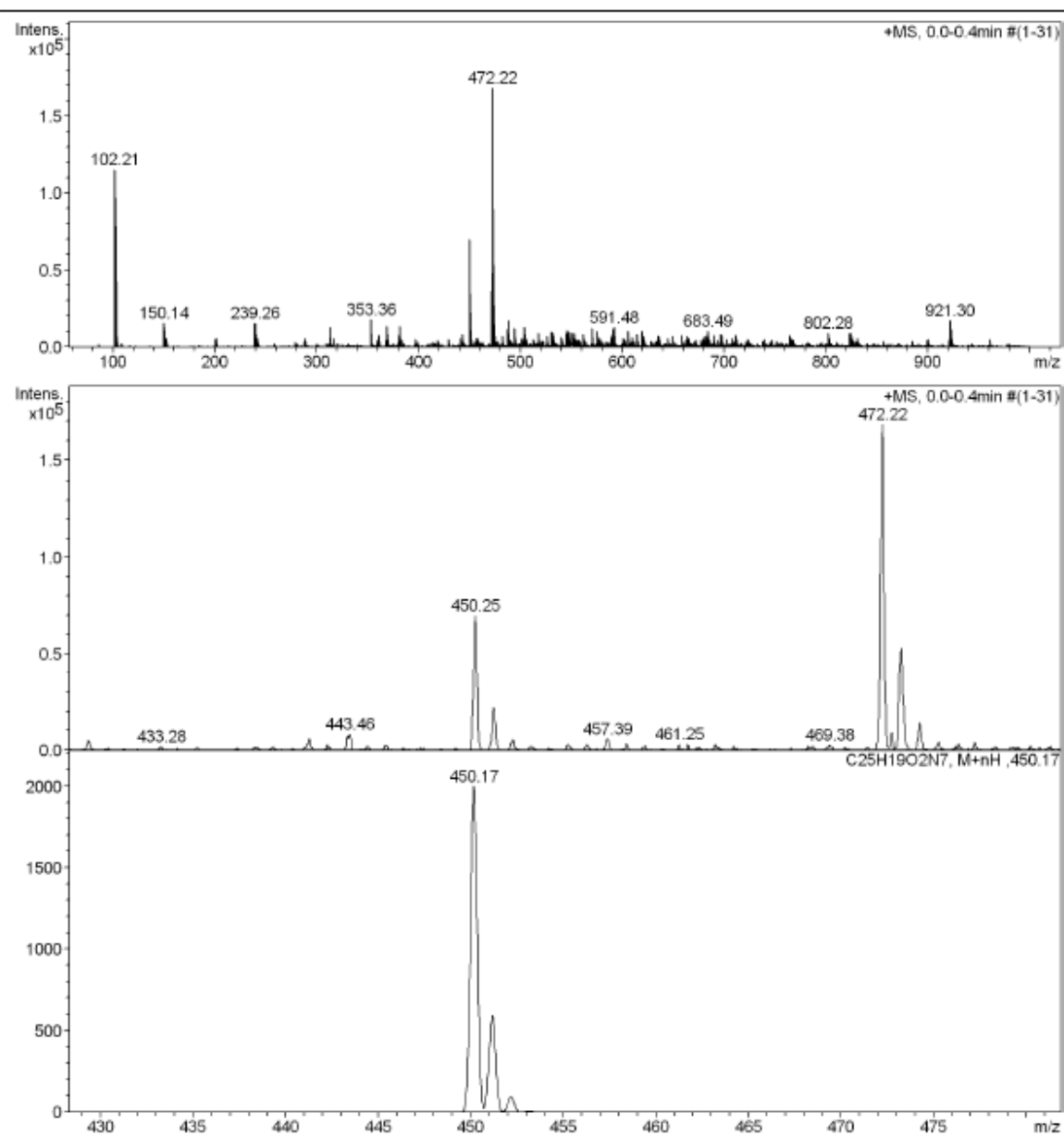**Figure S18**. Positive ion mode of ESI-mass spectrum of **C**.

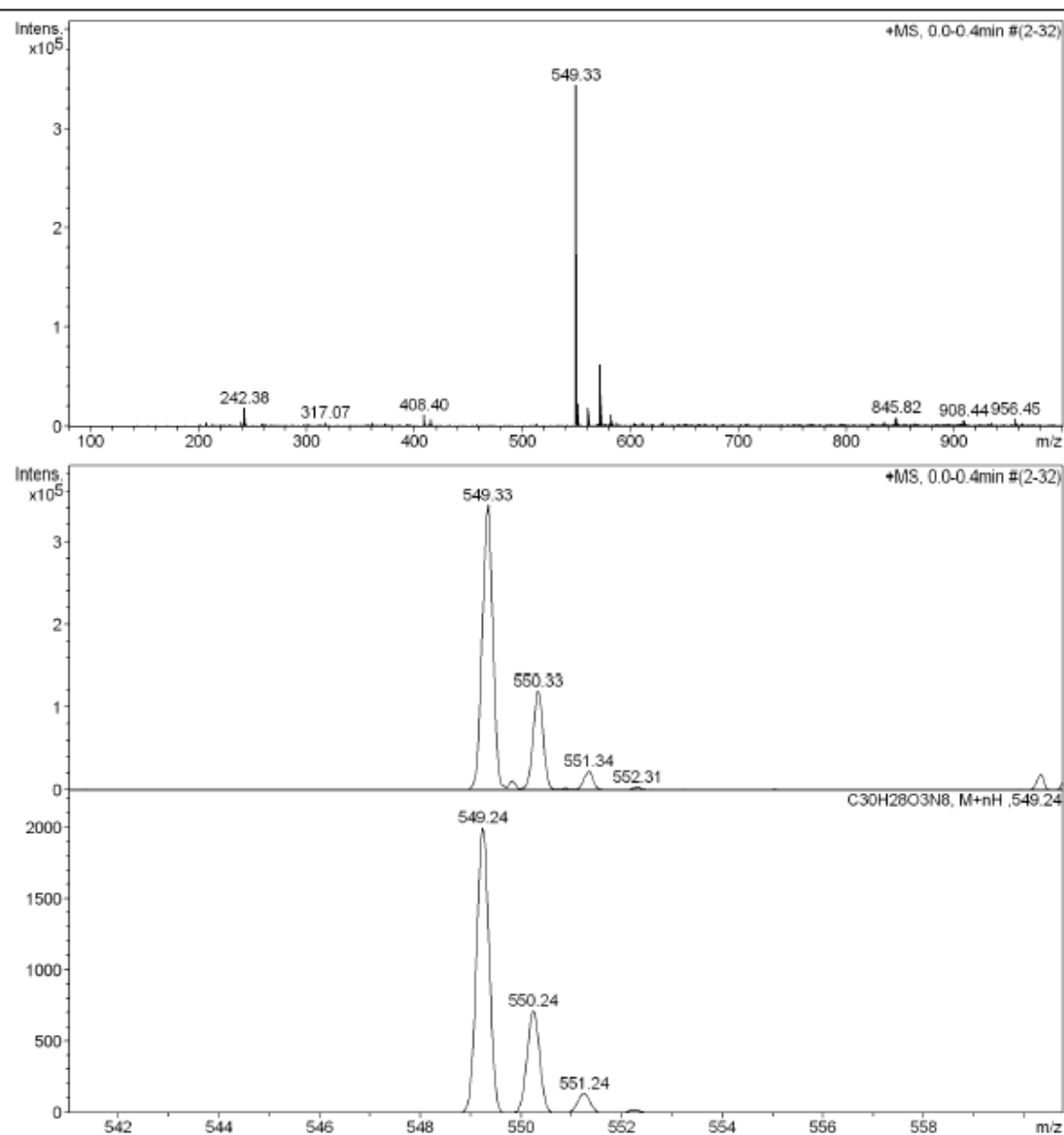**Figure S19.** Positive ion mode ESI-mass spectrum of **HL¹**.

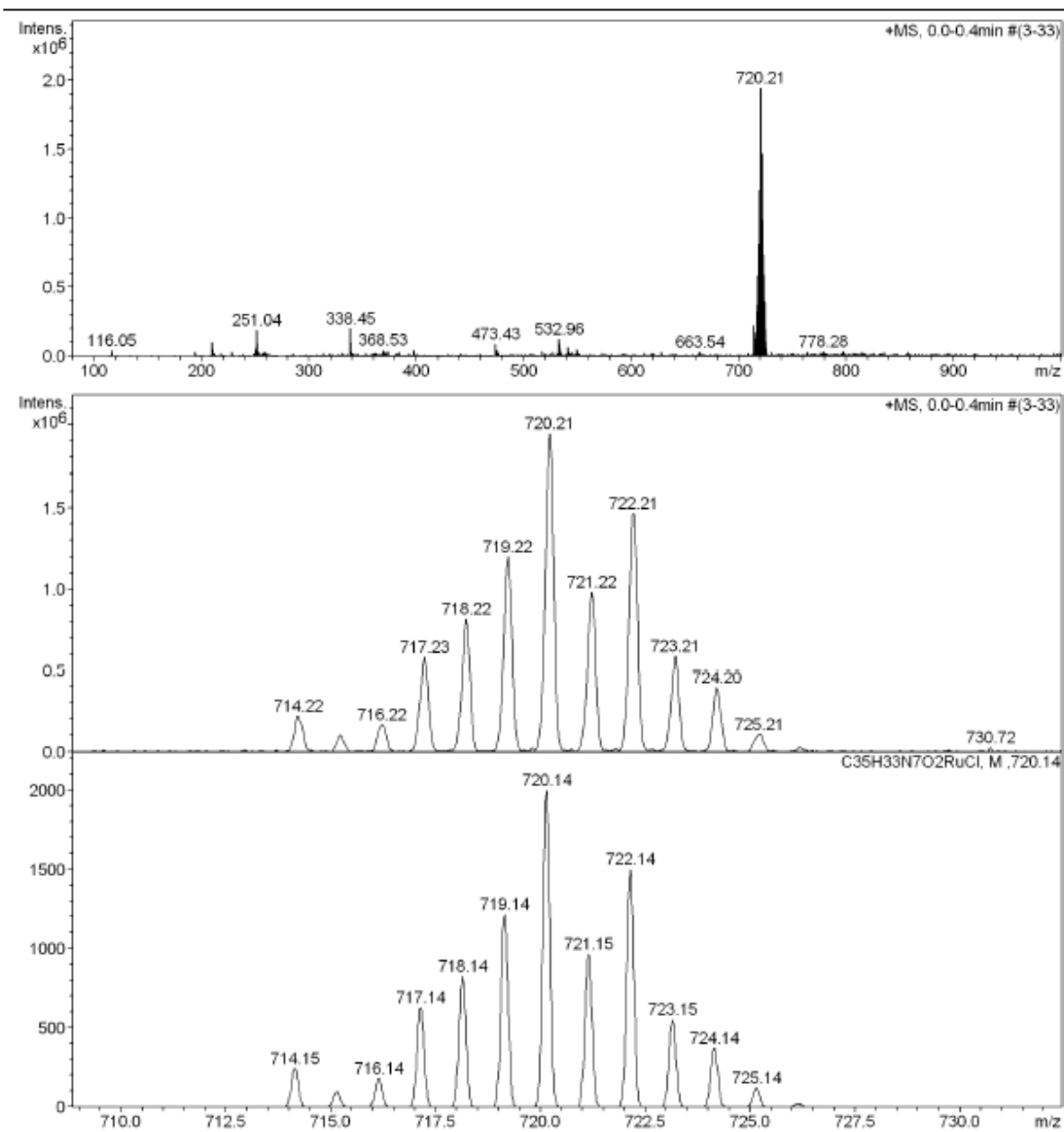**Figure S20.** Positive ion mode ESI-mass spectrum of **HL²**.

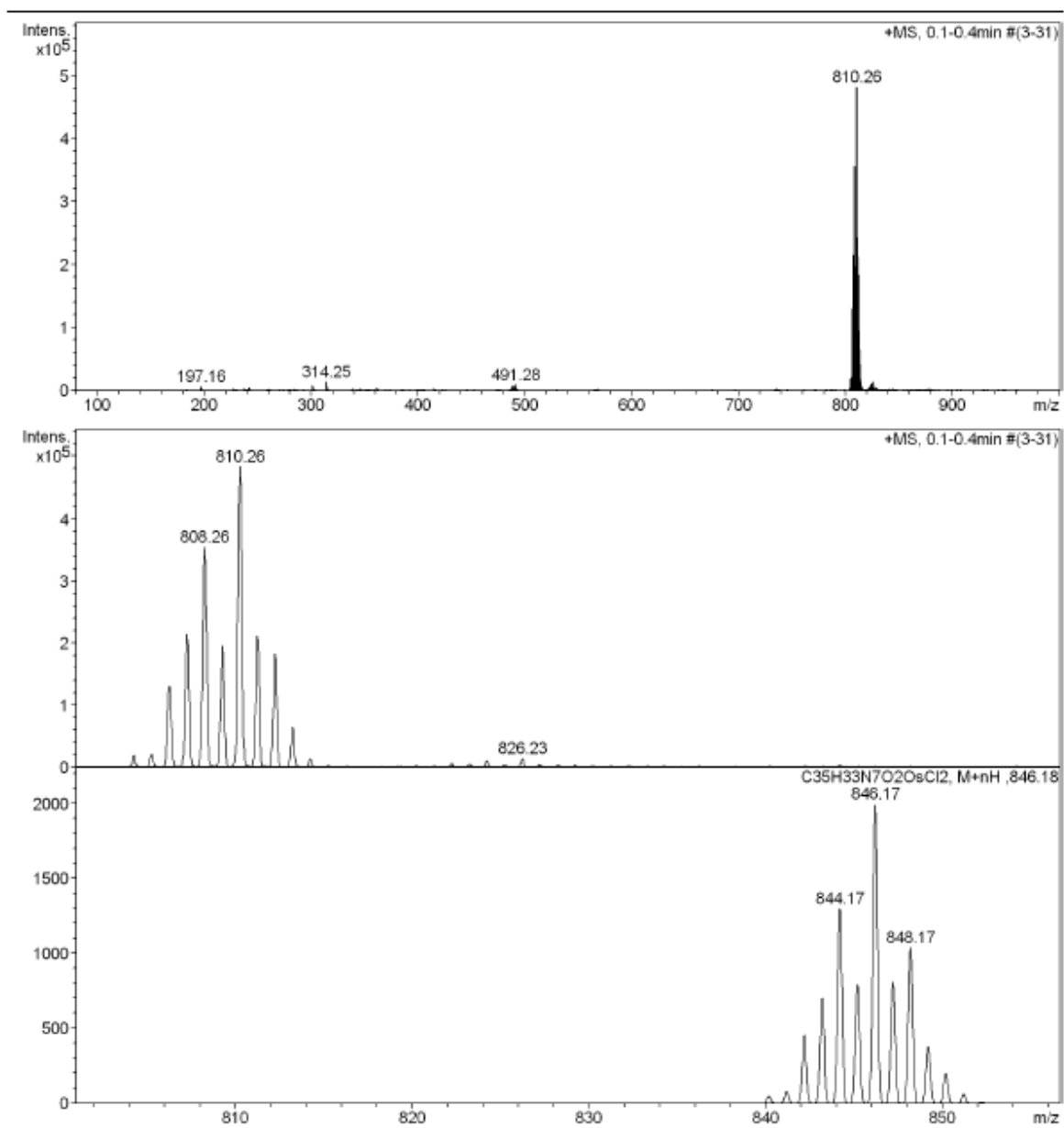**Figure S21.** Positive ion mode ESI-mass spectrum of **1**.
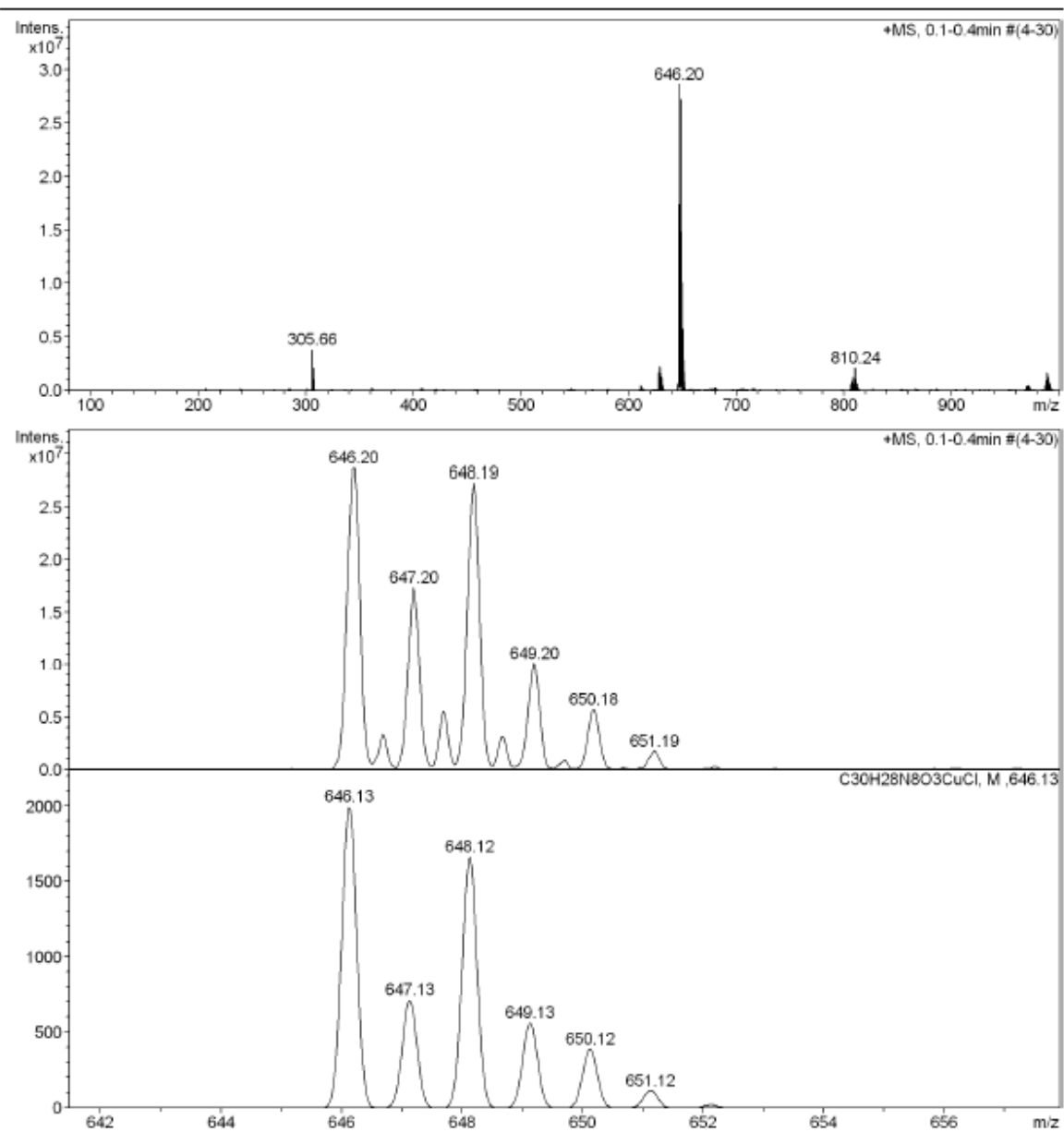
Figure S22. Positive ion mode ESI-mass spectrum of **2**.

Figure S23. Positive ion mode ESI-mass spectrum of **3**.

Molecular Docking

Table S3. The binding affinities as predicted by the scoring functions for the Pim1 kinase. **LI7** is the co-crystalized ligand. Root-mean-square deviation – RMSD from the co-crystalized ligand (heavy atoms) in Å.

Ligands	GS	CS	ChemPLP	ASP
B	51.6	32.3	69.6	40.0
A	44.9	33.7	66.5	35.8
LI7	50.5	31.4	58.0	28.4
RMSD:	0.9020	3.1517	0.5348	6.7059

Table S4. The molecular descriptors as calculated by QikProp and their corresponding Known Drug Indexes 2a and 2b (KDI$_{2a/2b}$).

	RB	MW(g/mol)	HD	HA	Log P	PSA (Å^2)	KDI$_{2A}$	KDI$_{2B}$
B	3	390.4	3	4.5	2.4	162.3	4.92	0.20
A	2	293.3	2	3.5	2.0	98.3	5.19	0.40

Table S5. Definition of lead-like, drug-like and Known Drug Space (KDS) in terms of molecular descriptors. The values given are the maxima for each descriptor for the volumes of chemical space used.

	Lead-like Space	Drug-like Space	Known Drug Space
Molecular weight (g mol^{-1})	300	500	800
Lipophilicity (Log P)	3	5	6.5
Hydrogen bond donors (HD)	3	5	7
Hydrogen bond acceptors (HA)	3	10	15
Polar surface area (Å^2) (PSA)	60	140	180
Rotatable bonds (RB)	3	10	17

Table S6. The single point and corrected zero-point vibrational energies (ZPE) of **B** in hartrees (a.u.).

Systems	Energy/a.u.	ZPE/a.u. [a]
B	−1362.24233	0.31450644
B$^{\bullet+}$	−1361.9785	0.31396035
B$^{\bullet-}$	−1362.2934	0.31071621
Fragment 1	−985.962007	0.24248527
Fragment 2	−376.173285	0.06496719

Corrected according to Wong[1]